BIOCHEMISTRY
including biophysical chemistry & molecular biology

Article

pubs.acs.org/biochemistry

Crystal Structure and Function of Human Nucleoplasmin (Npm2): A Histone Chaperone in Oocytes and Embryos

Olga Platonova,[†] Ildikó V. Akey,[†] James F. Head, and Christopher W. Akey*

Department of Physiology and Biophysics, Boston University School of Medicine, 700 Albany St., Boston, Massachusetts 02118-2526, United States

Supporting Information

ABSTRACT: Human Npm2 is an ortholog of *Xenopus* nucleoplasmin (Np), a chaperone that binds histones. We have determined the crystal structure of a truncated Npm2-core at 1.9 Å resolution and show that the N-terminal domains of Npm2 and Np form similar pentamers. This allowed us to model an Npm2 decamer which may be formed by hydrogen bonds between quasi-conserved residues in the interface between two pentamers. Interestingly, the Npm2 pentamer lacks a prototypical A1-acidic tract in each of its subunits. This feature may be responsible for the inability of Npm2-core to bind histones. However, Npm2 with a large acidic tract in its C-terminal tail (Npm2-A2) is able to bind histones and form large complexes. Fluorescence resonance energy transfer experiments and biochemical analysis of loop mutations support the premise that nucleoplasmins form decamers when they bind H2A-H2B dimers and H3-H4 tetramers simultaneously. In the absence of histone tetramers, these chaperones bind H2A-H2B dimers with a single pentamer forming the central hub. When taken together, our data provide insights into the mechanism of histone binding by nucleoplasmins.

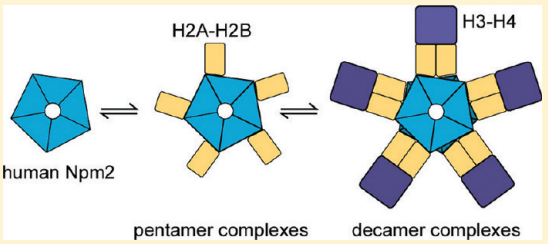

Npm2 is the mammalian ortholog of nucleoplasmin (Np), a well-characterized histone chaperone in *Xenopus* oocytes and early embryos.[1,2] Nucleoplasmin 2 expression is limited to oocytes, where it accumulates in nuclei and is excluded from nucleoli.[3] In mouse embryos, Npm2 is present until the 8-cell stage and is then down-regulated.[3] In *npm2*$^{-/-}$ mice there is a reduced cleavage of fertilized eggs to the two-cell stage, which renders these females less fertile. In addition, the architecture of cell nuclei is altered in knockout cells, as nucleoli appear fragmented and chromatin compaction is adversely affected. These defects persist in early zygotes.[3] Thus, Npm2 may function as a histone chaperone to help remodel chromatin in oocytes and early embryos,[3] but this has not been demonstrated directly. Interestingly, Npm2 does not appear to be required for sperm chromatin decondensation,[3] while Np plays an important role in this process in *Xenopus* eggs during fertilization.[2]

The general importance of histone chaperones is shown by the propensity of DNA to be damaged when nucleosome assembly is compromised, and conversely, free histones may also be detrimental to cells.[4] In *Xenopus* oocytes, Np may form storage complexes with H2A-H2B dimers while N1 associates with H3-H4 tetramers. Working in concert, these chaperones may direct nucleosome assembly in the early embryo.[5−7] Npm2 and Np have an overall sequence identity of ∼46%. Both chaperones contain a conserved N-terminal domain (the core), followed by a C-terminal tail that contains two acidic tracts (denoted A2 and A3), with a bipartite nuclear localization signal located between them (Figure 1A).[8] Acidic tracts in Np are disordered and play a role in binding core histones[9−11] and linker histones.[12] This includes a short acidic loop in the N-terminal domain (the A1-tract), which may interact with sperm basic proteins[13,14] and histones.[9−11]

Crystal structures have been determined for N-terminal domains of *Xenopus* Np and NO38[9,11,15] *Drosophila* NLP[10] and human Npm1.[16] This core domain is responsible for pentamer formation, and in three of the crystal structures, decamers are formed by the face-to-face association of two pentamers. In each decamer, salt bridges are formed by conserved residues in the AKDE and K-loops of opposing subunits in the two pentamers.[9,11,16] Pentamers and decamers in the Np family may each play a role in histone binding,[9−11,16] but the precise mechanism is currently being debated.[17−19]

In this paper, we present the crystal structure of a human Npm2-core pentamer. We then analyzed histone binding by Npm2-core and a longer version of the chaperone that contains a large acidic tract in the C-terminal tail (Npm2-A2). These studies show that hNpm2 requires the A2-tract to bind core histones. This is due to the fact that each A1-loop in Npm2 contains only a single acidic residue, which greatly reduces its electrostatic contribution to histone binding. We also made loop exchange mutants between Npm2 and Np to test the roles of the A1- and A2-tracts. On balance, we find the A1- and A2-tracts of Np may act synergistically in histone binding. We also show that Npm2 and Np form decamers when they bind the four core histones, while H2A-H2B dimers bind to a single pentamer. We then modeled an Npm2 decamer to reveal compensatory changes in residues of the AKEE and Q-loops of

Received: April 30, 2011
Revised: July 24, 2011
Published: August 24, 2011

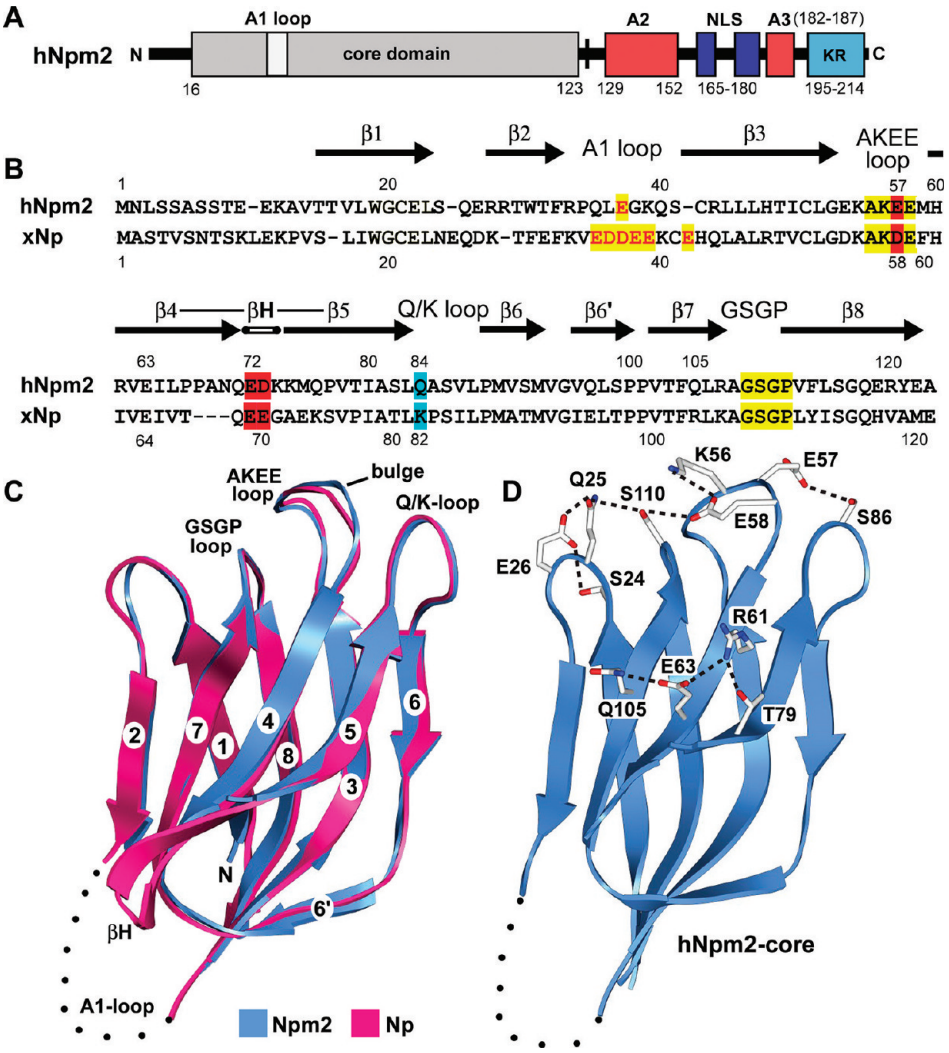

Figure 1. Domain organization, sequence alignment, and monomer structure of Npm2. (A) The domain architecture of Npm2 is shown with acidic tracts colored in red, the bipartite NLS in blue, and a C-terminal, basic KR-rich region in light blue. (B) A sequence alignment for Npm2- and Np-core domains is shown with β-strands indicated by black arrows. Important loops are highlighted in yellow, acidic residues are shown in red, and additional residues that may participate in decamer formation are highlighted in cyan. (C) The Npm2-core subunit is shown as a ribbon diagram (in blue), overlaid onto Np-core (in red). The position and approximate size of the A1-loop are indicated by a dotted loop, and the β-hairpin of Np is labeled (βH). A bulge in the AKEE-loop is present relative to the equivalent AKDE-loop of Np. (D) A salt bridge network extends across the top surface of the Npm2-core domain. In addition, hydrogen bonds are also present between Glu57 and Ser86, and a second network is formed on the external face centered on Glu63. Ribbon figures were made with Chimera.[37]

this chaperone. These residues may form hydrogen bonds between opposing pentamers when chaperone decamers are formed during histone binding. Finally, we present FRET and biochemical data to support a model in which H2A-H2B dimers bind directly to nucleoplasmins, followed by the addition of H3-H4 tetramers at higher radius to form larger complexes.

EXPERIMENTAL PROCEDURES

Cloning and Chaperone Expression. The human Npm2 gene in pET23[3] was used to create all hNpm2 variants using the QuikChange XL site-directed mutagenesis kit (Stratagene). For hNpm2-A2 (M1-D152), a stop codon was inserted after Asp152. The hNpm2-core domain (T15-E122) was created by inserting NdeI and Hind III restriction endonuclease sites at the 5′ and 3′ ends using PCR. The resulting core fragment was subcloned into the T7 expression vector pRK172. Full length Np DNA in pRK172 was modified to create all Np variants. First, a truncated N-terminal domain was created by removing Ala2-Lys10. Np-A2 (Np11−149) and cNp (11−124) were created by inserting double stop codons after residues Ser149 and Tyr124, respectively. A1-loop mutants of hNpm2-A2 and Np-A2 were created by exchanging the A1-loop sequence (Q^{35}LEGK) of Npm2 with the A1-tract sequence of *Xenopus laevis* Np (E^{35}DDEE). This substitution was also introduced into the hNpm2- and Np-core constructs. Two different AKDE-/K-loop double mutants of Np-A2 were also created: Np-A2 (AKDE to AGGG and K82S) and Np-A2 (AKDE to AGEE and K82E). With the exception of hNpm2-core, all proteins were constitutively expressed at 37 °C overnight (18 h) in *E. coli* BL21(DE3) cells using 2xYT media supplemented with 0.5% glycerol, 0.2% lactose, and 2 mM $MgCl_2/MgSO_4$.[20] hNpm2-core cells were grown in LB medium at 37 °C and induced with 1 mM IPTG for 3 h.

hNpm2 and Np Purification. For Npm2, pelleted cells were resuspended in 50 mM Tris-HCl pH 8, 100 mM NaCl, 5 mM EDTA, 5 mM 2-mercaptoethanol, and 1 mM PMSF and

dx.doi.org/10.1021/bi2006652 | *Biochemistry* 2011, 50, 8078−8089

then lysed with lysozyme and deoxycholic acid.[9] Lysates were spun at 100000*g*, the supernatant was again treated with lysozyme (2 mg/mL) for 30 min on ice to facilitate DNA precipitation, and the solution was cleared with a second high speed spin. Supernatants were treated at 80 °C for 10 min and denatured proteins removed by centrifugation. Heat stable hNpm2-core was applied to a 1 mL HiTrap CM FF column (GE Healthcare) equilibrated with 50 mM Na_2HPO_4, pH 6.0, 100 mM NaCl, and 5 mM β-mercaptoethanol. Protein was eluted using a 0.1−1.0 M NaCl gradient; fractions were pooled, dialyzed against buffer containing 25 mM Tris-HCl pH 7.5, 100 mM NaCl, and then concentrated using a Centriprep YM-10 (Millipore) to 16 mg/mL for crystallization. Supernatant containing hNpm2-core with the *Xenopus* A1-tract was processed similarly using a 1 mL HiTrap DEAE FF column (GE Healthcare) equilibrated in 50 mM Na_2HPO_4, pH 7.5, 100 mM NaCl, and 5 mM β-mercaptoethanol. Extracts of hNpm2-A2 with and without the *Xenopus* A1-tract substitution were brought to 60% saturation with AMS and spun to remove precipitated contaminants. Proteins were then precipitated by adjusting the pH to ∼4.5 with 1 N HCl, resolubilized, and further purified on a HiTrap DEAE FF column as above.

To purify *Xenopus* Np, cells were lysed in buffer containing 50 mM Na_2HPO_4 pH 8.0, 100 mM NaCl, 5 mM $MgCl_2$, 1 mM EDTA, and 1 mM PMSF using the lysozyme/deoxycholic acid method. Soluble proteins were heated to 80 °C for 10 min and centrifuged to remove precipitated material. Np-A2 was brought to 80% saturation with AMS and spun to remove precipitants, and the pH was decreased to ∼4.5 using 1 N HCl to precipitate soluble Np-A2. The protein was resolubilized in 50 mM Na_2HPO_4 pH 8.0, 100 mM NaCl, applied to 1 mL HiTrap CM FF and HiTrap DEAE FF columns (GE Healthcare) linked in tandem, and then eluted from the anion exchange resin using a NaCl step gradient in 25 mM Tris-HCl pH 7.5 with salt concentrations increased in 0.2 M increments. Np-A2 and its variants eluted with 0.4 M NaCl and purified proteins were concentrated using a Centriprep YM-10.

Np-core and the A1-loop exchange mutant were purified following the 80 °C heat treatment by passing them over DEAE-DE52 resin (Whatman) equilibrated with 25 mM Tris-HCl pH 7.5, 0.1 M NaCl. Both proteins were eluted with a NaCl step gradient at 0.4 M NaCl. Purified Np-core was concentrated by the addition of 80% AMS and then lowering the pH to about 4.5, while the A1-loop mutant precipitated with 80% AMS. All chaperones were flash frozen in liquid nitrogen and stored at −80 °C. A native gel of purified chaperones is shown in Figure 1 of the Supporting Information. The overall mobility of each chaperone is generally consistent with the number of acidic residues in their acidic tracts and is modulated by changes in hydrodynamic radii.

Histone Purification. Core histones were purified from chicken erythrocytes[21] with the following modifications. Lysed nuclei released a highly compacted chromatin nucleoid that was visualized under a light microscope (i.e., chromatin balls). Chromatin content was quantitated using a Neubauer hemocytometer, and the concentration adjusted to ∼1.5 × 10^6 chromatin balls/mL. To 30 mL of chromatin balls, Tris-HCl pH 8.5 was added to a final concentration of 30 mM, and $CaCl_2$ and PMSF were added to 1 mM; micrococcal nuclease (Worthington Biochemical Corp.) was then added to 5 units/mL. The sample was prewarmed at 37 °C for 5 min, heparin sulfate was added to 1 mg/mL, and the sample was incubated 30 min at 37 °C. The digestion was stopped by adding EDTA to 2 mM, and the sample was centrifuged at 4000*g* for 15 min at 4 °C to generate soluble long chromatin. Core histones were purified either as dimers, tetramers, or a mixture using hydroxyapatite (Bio-Gel HTP, Biorad). The resin-to-histone ratio was critical for efficient histone recovery; hence, the histone concentration of long chromatin was quantitated using the Bradford assay prior to resin binding. Hydroxyapatite (HA) was used as a 25% slurry in 50 mM $NaPO_4$ pH 5.0, 65 mM NaCl, and the long chromatin was added at a ratio of 1 g HA per 6 mg histones and incubated for 2 h at room temperature. Resin was settled with centrifugation and washed twice with the slurry buffer. Linker histones were eluted with 50 mM $NaPO_4$ pH 5.0, 650 mM NaCl, dimers were eluted with 1 M NaCl, and tetramers were eluted with 2 M NaCl after dimer removal. A core histone mixture was purified with a single 2 M NaCl elution. Histones were concentrated using 60% AMS precipitation and then resolubilized in 50 mM $NaPO_4$ pH 6.0, 2 M NaCl. These proteins were then flash frozen in liquid nitrogen and stored at −80 °C.

Reconstitution of Chaperone−Histone Complexes and FRET Experiments. Protein concentrations were determined based on A_{280} measurements using calculated extinction coefficients and the histone−chaperone complexes were reconstituted at empirically determined protein ratios, as excess histones led to aggregation. Np−histone complexes were reconstituted by mixing the proteins in the presence of 1 M NaCl and desalting them together through a G25 spin column.[9] The spin column was equilibrated in 25 mM Tris-HCl pH 7.5 and 100 mM NaCl for Np-core proteins and in 100 mM Tris-HCl, pH 7.5 and 100 mM NaCl for Np-A2 proteins. Since histone complexes with hNpm2 were more prone to aggregation, individual proteins were first desalted over 1 mL Sephadex-G25 (GE Healthcare) spin columns equilibrated in 100 mM Tris-HCl pH 7.5 and 100 mM NaCl. However, hNpm2-A2 with the *Xenopus* A1-loop aggregated in Tris buffer, so this protein was desalted into 25 mM HEPES-NaOH pH 7.5 and 100 mM NaCl. The approach of using desalted proteins during reconstitution allowed better control of component ratios in the complexes. In addition, glycerol (5%) was also added during complex formation. Glycerol gradients in the appropriate buffer (10%−40%; 2.2 mL per tube) were used to assess complex formation.[11] Gradients were spun in a Sorval RP55S rotor (55 000 rpm and 17 °C) for 5 h 45 min, and in total, 15 fractions were harvested from the top. Separation of proteins by SDS-PAGE was done on discontinuous Tris-glycine gels, and native gels were run similarly but without SDS.

For FRET experiments, a cysteine mutant of hNpm2-A2 was designed for labeling with sulfhydryl-reactive fluorophores, by moving Cys42 to position 40 within the A1-loop (EGKQSCR to EGKCQSR) to make it more accessible for labeling. This mutation should not have affected the thermostable pentamer since Cys42 is not buried in the hydrophobic core and the Dylight649 labeled chaperone ran as a pentamer on a native gel (Supporting Information Figure 1, rightmost lane). Expression and purification were similar to that used for wild-type hNpm2-A2, with the exception that 5 mM β-mercaptoethanol was present at all steps. Np chaperones were labeled similarly at Cys41. Prior to labeling, chaperones were reduced with 10 mM tris-(2-carboxyethyl)phosphine (TCEP; Molecular Probes) for 30 min at 22 °C and then spun through a Sephadex-G25 column equilibrated in 50 mM Na_2HPO_4, pH 7.5, 100 mM NaCl,

2.5 mM EDTA. Histones were similarly desalted. Chaperones were labeled with either DyLight 549-malemide or DyLight 649-malemide (Thermo Scientific). The conjugation reaction mixture contained 100 μL of chaperone at 0.5 mM in phosphate buffer and 11 μL of fluorophore at 10 mg/mL in DMSO. The reaction proceeded at ∼22 °C overnight. Excess fluorophore was removed by exhaustive dialysis against 25 mM Tris-HCl, pH 7.5 and 100 mM NaCl in the dark. Histone dimers and tetramers were labeled with either the amine-reactive fluorophore DyLight 549-NHS or DyLight 649-NHS (*N*-hydroxysuccinimide ester). These conjugation reactions were allowed to proceed for 1 h, again followed by exhaustive dialysis. The extent of protein labeling was evaluated by determining the protein (based on A_{280}) and fluorophore (based on A_{max}) concentrations using their extinction coefficients and calculating the ratio of moles of dye per moles of protein. A typical labeling efficiency was ∼0.4 mol of dye per chaperone subunit. However, the labeling efficiency for Npm2-A2, Np-core, and Np-A2 varied between 0.2 and 0.6 and also differed for donor and acceptor pairs. Histone labeling efficiency was also ∼0.4−0.6 per dimer and tetramer, respectively. At this pH, the labeling may be directed primarily toward N-terminal amino groups. As shown in Supporting Information Figure 1A, labeling of Npm2-A2 and Np-core did not perturb their pentameric structures.

Complexes were reconstituted by mixing components in equimolar histone−chaperone ratios at 1 μM concentration for each of the components, followed by incubation for 30 min at ∼22 °C. Donor molecules (DyLight-549) were excited at 557 nm (2.0 nm bandpass), and emission spectra from the acceptor (DyLight-649; 2.0 nm bandpass) were recorded at ambient temperature using a FluoroMax-2 spectrofluorimeter (Instruments SA, Edison, NJ) and plotted with Excel after subtraction of buffer background and a dilution correction. Each experiment was repeated 2−3 times with a typical variation of at most ∼5% in the intensity readings.

Human Npm2-Core Crystallization, Structure Determination, and Refinement. Crystallization experiments were carried out with the hanging drop method using Linbro plates with 2 μL of hNpm2-core (8 mg/mL) and 2 μL of mother liquor in the drop and 0.5 mL of mother liquor in the well. Crystals with a square or rectangular morphology were obtained in 20% (v/v) PEG 3350, 100 mM NaCl, 25 mM Tris-HCl, pH 7.5. Data sets were collected on beamline X8C at the NSLS and processed with the HKL2000 program suite.[22] The structure was solved in space group $P2_1$ by molecular replacement with EPMR,[23] using an Np pentamer (1K5J) as the reference. The EPMR solution showed two pentamers per asymmetric unit, and resulting models were then mutated to the hNpm2-core sequence. Initial rigid body refinements gave an R_{free} of 0.38. At this point, the complete hNpm2-core subunit could be traced with the exception of the A1-loops and β-hairpin turns. This model was subjected to positional refinement with strict NCS restrains in CNS[24] followed by rebuilding in Coot.[25] Cycles of simulated annealing with restrained refinement, B-group refinement, and water picking were performed in PHENIX,[26] alternating with rebuilding in Coot. The resulting model was verified by manual inspection. All of the A1-loops and β-hairpin turns were disordered in the final model. Refined pentamer models were validated using PROCHECK,[27] and no residues were in the disallowed region of the Ramachandran plot. Molecular graphics were made with Chimera.[37]

RESULTS

Structure of the Human Npm2 Monomer and Pentamer. Initially, we expressed full length human Npm2 in *E. coli*, and these molecules were clipped after the A2-tract by endogenous proteases (see Figure 1A). On the basis of the known flexibility of the C-terminal tail in Np-family members, we then cloned and expressed the N-terminal core domain. This region readily crystallized in space group $P2_1$ with two pentamers per asymmetric unit. The structure was solved at 1.9 Å by molecular replacement using an Np-core pentamer as a search model (1K5J). Final refinement statistics are given in Table 1. As expected, the Npm2 oligomerization domain is an 8-stranded β-barrel and Cα main-chain atoms of aligned Npm2- and Np-core subunits have a calculated rmsd of 0.61 Å. The positions of β-strands are shown on a sequence alignment (Figure 1B), and overlaid Npm2- and Np-core subunits are presented in Figure 1C.

A number of features in the Npm2-core structure are of interest. First, a prominent β-hairpin in the Npm2 subunit is three residues longer than in Np and residues Ala68-Gln76 are disordered (Figure 1A,B), as they generally are for Np subunits.[9,15] Second, the A1-loop of Npm2 contains a single acidic residue (Glu37), rather than multiple acidic residues (3−12) that are present in other Np-family members. The A1-loop is located between strands β2-β3 and is disordered in all subunits. Third, there is a bulge in the AKEE loop (equivalent to AKDE in Np) that may play a role in decamer formation. Fourth, an extended salt bridge network is anchored by Lys56 and Glu58 of the AKEE loop and involves Ser110, Gln25, Glu26, and Ser24 (Figure 1D). Fifth, Glu57 in the AKEE loop makes a hydrogen bond to Ser86 in the adjacent Q-loop. Finally, a highly conserved glutamate on the β-hairpin (Glu63) makes a hydrogen bond with

Table 1. Crystal Information, Data Collection, and Refinement Statistics[a]

crystal data	
space group	$P2_1$
unit cell (Å)	49.0 107.2 108.7
unique angle (deg)	β = 102.5
asymmetric unit (asu)	two pentamers
residues	862
reflections	82427
data cutoff	$F > 0$
R_{merge}[a]	0.05 (0.265)
% completeness	95.5
$I/\sigma(I)$	18.4 (6.4)
refinement statistics	
resolution	40.5−1.9
R_{Cryst}/R_{Free}	0.19/0.24
rms deviations	
bond lengths (Å)	0.012
bond angles (deg)	1.37
mean *B* value (all atoms)	33.4
waters/asu	305
Ramachandran plot	
core areas (%)	89.3
additional allowed areas (%)	10.7

[a]In the outermost shell.

dx.doi.org/10.1021/bi2006652 | *Biochemistry* 2011, 50, 8078−8089

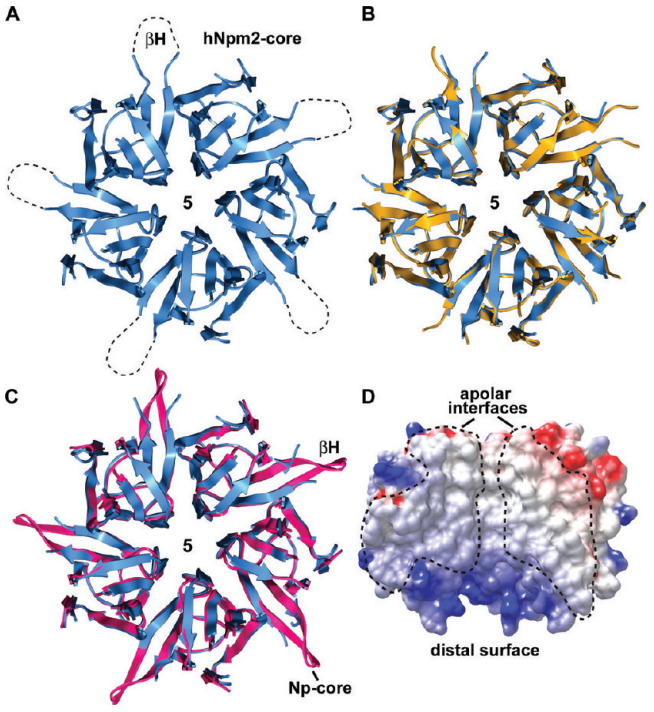

Figure 2. Npm2- and Np-core pentamers. (A) The Npm2-core pentamer is shown as a ribbon representation viewed from the top. Approximate positions of β-hairpin tips are indicated with dotted loops, since they are not well ordered. (B) Two independent Npm2-core pentamers in the asymmetric unit are overlaid. (C) A perfect Np-core pentamer with 5 β-hairpins (in red)[9] is shown overlaid with the human Npm2-core pentamer from panel A (in blue). (D) An electrostatic surface is shown of three adjacent subunits within the Npm2-core pentamer. The exposed subunit−subunit interface is nonpolar (see dashed outlines).

Gln105 and Arg61 to form an extended network that includes Thr79. A similar interaction occurs in Np between Glu64 and Arg105.[9]

The asymmetric unit in the $P2_1$ crystal contained two Npm2-core pentamers, but these molecules did not form a decamer. After aligning the two Npm2-core pentamers (Figure 2A,B) and excluding flexible β-hairpins, the rmsd for main chain atoms was 0.33 Å. As expected, human Npm2- and Np-core pentamers share a conserved subunit packing within their respective pentamers (Figure 2C). In a previous paper, a complete β-hairpin was built into density for one subunit in the Np-core crystal structure.[9] When this Np-core subunit was repeated 5 times in a ring, it created a "perfect" pentamer with five extended β-hairpins (red pentamers in Figure 2C). By comparison, the β-hairpin of Npm2-core may be kinked due to the presence of consecutive proline residues (Pro66, Pro67) and is then completely disordered for the next 8−9 residues in a region that includes the β-turn. These flexible β-hairpins could play an important role in histone binding, since they are located on lateral surfaces of their respective pentamers (see next sections). Intriguingly, a pair of conserved acidic residues is located at the tips of the β-hairpins (Figure 1B) where they could interact with basic histones.

Finally, the Npm2 pentamer is formed by subunits that interact through a mostly hydrophobic interface. This interface is shown in a cutaway view with two subunits removed from the pentamer (Figure 2D). The Npm2-core pentamer is markedly thermostable because no unfolding could be detected to at least 96 °C by circular dichroism (not shown). This property is shared with Np[9,15] and may arise in part from the apolar nature of the subunit interface in the pentamer.

Histone Binding to Human Nucleoplasmin. We next tested the hypothesis that Npm2 may function as a histone chaperone. As a control, Np-core histone complexes with H2A-H2B dimers and H3-H4 tetramers were run on a glycerol gradient. These large complexes peaked in fractions 10−11 and have a calculated molecular weight of ~680 kDa, based on our model (Figure 3A).[9] GroEL (800 kDa) was used as a molecular standard and ran in fraction 12 (not shown). In addition, histone dimers and tetramers remained at the top of the gradient in the absence of a chaperone (not shown). As reported previously, the ratio of histone dimers and tetramers

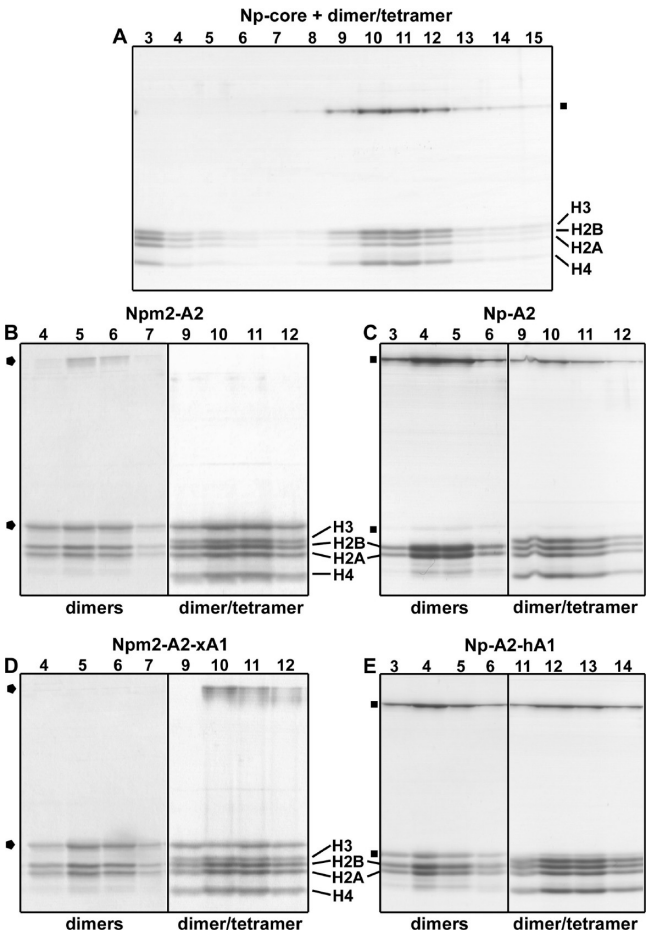

Figure 3. Histone binding by Npm2 and Np. (A) Np-core binds all four core histones. The Np chaperone may run as a monomer or pentamer, depending upon the ligand and buffer conditions, and is marked with a black square on these gels. In this experiment, Np remained as intact pentamers in SDS after boiling. (B) Human Npm2-A2 binds histone dimers (left panel) or a mixture of dimers and tetramers (right panel). Only peak fractions from the glycerol gradients are shown. The position of Npm2 chaperone is marked with a black pentagon for both monomers and pentamers in these panels. (C) Np-A2 forms large complexes with histone dimers (left panel) or dimers and tetramers (right panel). (D) Npm2-A2 with the A1-tract of Np binds histone dimers (left panel) or dimers and tetramers (right panel). (E) Np-A2 with the A1-loop of Npm2 binds histone dimers (left panel) or dimers and tetramers (right panel).

dx.doi.org/10.1021/bi2006652 | *Biochemistry* 2011, 50, 8078−8089

in the complex appears to be ~1:1.[9] We then mixed all four core histones with Npm2-core and ran them on a glycerol gradient. Remarkably, the Npm2-core pentamer did not bind histones; instead, the proteins remained at the top of the gradient with some smearing due perhaps to nonspecific interactions (not shown). The inability of Npm2-core to bind core histones in the normal way may reflect a paucity of acidic residues in the A1-loop, since this feature has only one acidic residue (Glu37). By comparison, Np-core has 5 acidic residues in the A1-tract (E_{35}DDEE$_{39}$, Figure 1B).

This result suggested that Npm2 might use A2- and A3-tracts in the C-terminal tail to promote histone binding (Figure 1A). Since we could not express a full length Npm2 in bacteria, we engineered a protein that contained the larger A2-tract in the C-terminal tail. After purification, Npm2-A2 was able to bind the four core histones and form large complexes (Figure 3B, right panel), in a manner similar to Np.[9] We also found that Npm2-A2 bound histone dimers to form smaller complexes, based on their migration on a glycerol gradient (Figure 3B, left panel). As a positive control, we engineered a truncated Np-A2, and this chaperone was used to form complexes with core histones. The mobility of the Np-A2 histone complexes was similar to those formed with Npm2-A2, when using histone dimers and tetramers (Figure 3C, right panel) or just dimers (Figure 3C, left panel). On the basis of these experiments, we concluded that Npm2 requires the A2-tract to bind core histones, whereas Np-core is able to bind histones by using acidic residues in the A1-tract.[9]

We then made a series of loop exchange mutants to test the role of acidic residues in the A1-tract. First we engineered an Npm2-core which contained the A1-tract of Np. This mutant Npm2-core bound all four core histones weakly when the complexes were run on glycerol gradients (not shown). In the reverse experiment, Np-core with the A1-loop of Npm2 lost the ability to bind histones and form specific complexes (not shown). Next, we made an Npm2-A2 chaperone that contained the A1-tract of *Xenopus* Np. This chimeric chaperone bound histone dimers and tetramers (Figure 3D, right panel) or dimers (Figure 3D, left panel). Conversely, an Np-A2 chaperone with the A1-loop of Npm2 retained the ability to bind histone dimers and tetramers (Figure 3E, right panel) or dimers by themselves (Figure 3E, left panel). However, there was a tendency for chimeric Np-A2 with bound histone dimers and tetramers to aggregate a bit, as reflected by the greater mobility of these complexes in the gradient (Figure 3E, right panel).

When taken together, these experiments highlight the importance of the acidic tracts in histone binding. In particular, the A2-tract is required for histone binding by Npm2. Our data also suggest that the A1- and A2-tracts of Np act synergistically in histone binding. This may be a general feature of all Np family members that have a functional A1-tract.[10,11] Importantly, Np and Npm2 both form complexes with histone dimers. In addition, each chaperone interacts with histone dimers and tetramers to create larger complexes with a similar histone stoichiometry. These data are consistent with the hypothesis that Npm2 may function as a histone chaperone in cells, even though it lacks the prototypical A1-tract. While the role of the smaller A3-tract is not known (Figure 1A), it may further stabilize histone complexes with nucleoplasmins.

Nucleoplasmins Form a Central Hub for Core Histones. Previous studies of Np family members suggested that a chaperone decamer may bind histones to form large complexes that contain histone octamers. This hypothesis was based on sedimentation analysis,[9] the observed 1:1 ratio of H2A-H2B and H3-H4 in these complexes, coupled with the mobility of these complexes on a calibrated molecular sizing column[9,10] and on glycerol gradients[11] (this work). To further define the mechanism of histone binding, we wanted to demonstrate that two chaperone pentamers are present within the larger histone complexes that contain all four core histones. We also asked the question: do H2A-H2B dimers bind to a chaperone pentamer in the absence of H3-H4 tetramers?

To answer these questions, we used fluorescence resonance energy transfer (FRET) experiments to monitor decamer formation. First, we labeled Cys41 of Np-core with either DyLight 549, a malemide-activated donor, or DyLight 649, an acceptor dye. Cysteine 41 contains the only solvent accessible SH group in the Np-core subunit and is located adjacent to the A1-tract on the distal face of the pentamer (Figure 1B).[9] The distance between dye molecules on the two distal faces of the decamer is ~80 Å. Hence, dye molecules should show a FRET signal if donor and acceptor labeled pentamers interact to form a decamer. Equal amounts of the two labeled Np-A2 pentamers were mixed together (final concentration 1 μM), and enhanced emission by DyLight 649 was monitored as a function of histone addition, relative to a background curve for Np without added histones. First, we added H2A-H2B dimers and saw only a small and broadly distributed increase in the signal (Figure 4A, light gray curve). However, a FRET peak was observed when similar amounts of H2A-H2B dimers and H3-H4 tetramers were added to Np-A2 (black curve, Figure 4A). Importantly, the magnitude of the signal was consistent with decamer formation given the labeling efficiency, label geometry, and the number of possible decamers in the population that would be doubly labeled (50%). Under similar conditions, labeled Npm2-A2 proteins also gave a clear FRET signal with bound histone dimers and tetramers (Figure 4B, left), but not with histone dimers by themselves (not shown). We then made Np-A2 complexes with an equimolar mixture of histone dimers and tetramers and added NaCl to a final concentration of 1 M. Under these conditions, we found that the fluorescence peak was lost as the complexes disassembled (see hatched bar, Figure 4B, middle). When taken together, glycerol gradient and FRET experiments suggest that Np and Npm2 may each form decamers when histone dimers and tetramers are bound to these chaperones at the same time. Under these conditions, the ~1:1 ratio of the core histones indicates that H2A-H2B and H3-H4 may form octamers. In addition, only a diffuse fluorescence signal was obtained when histone dimers were bound to either of the nucleoplasmins. This suggests that H2A-H2B dimers may bind to chaperone pentamers rather than to decamers. This idea is consistent with glycerol gradients on the various complexes (Figure 3B,C) and agrees with solution X-ray scattering experiments on Np H2A-H2B complexes.[18]

Since Np-A2 proved to be a more robust molecule for mutation and bacterial expression, we asked whether Np-A2 could form decamers after mutating residues in the AKDE and K-loops. These residues form salt bridges in the interface between opposing pentamers. First, we engineered a double loop mutant in which charged side chains were replaced with small uncharged side chains (AKDE to AGGG and K82S). After purification, core histones were added to the Np-A2 double loop mutant and proteins were run on glycerol

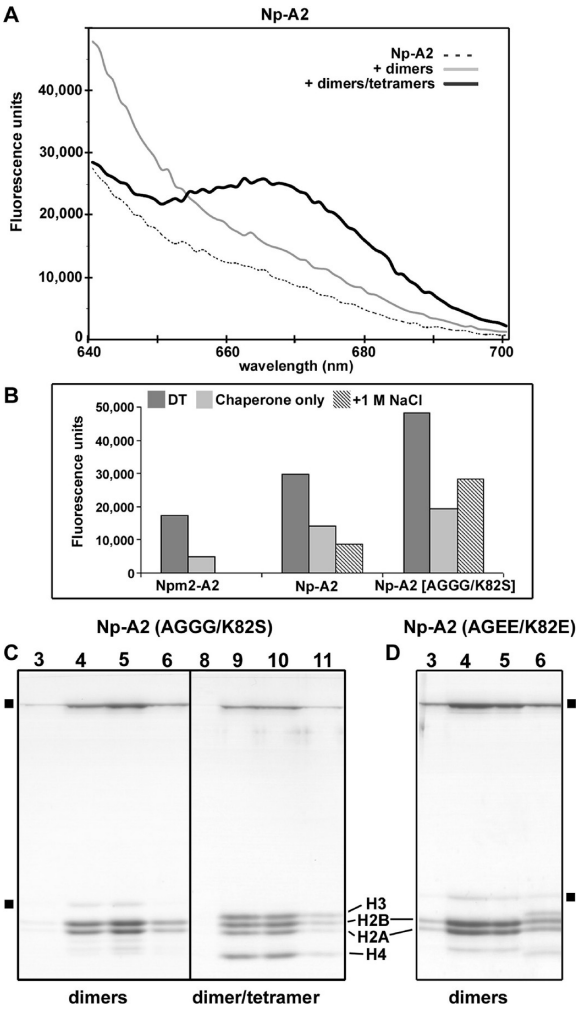

Figure 4. The role of chaperone decamers in binding core histones. (A) Np-A2 pentamers with appropriate donor and acceptor dyes were mixed and addition of histone dimers and tetramers gave a FRET peak. The binding of histone dimers alone gives a rather flat signal attributed to nonspecific aggregation. The chaperone by itself is shown with a dashed line. Data for a typical experiment are shown. However, all experiments were done three times with less than a 5% variation in the observed intensities. (B) A histogram is shown for similar FRET studies in which two labeled pools of a chaperone were mixed and then unlabeled core-histones were added (DT). The plotted data include results for Npm2-A2, Np-A2, and a double loop mutant of Np-A2 (AKDE to AGGG and K82S). The absolute intensity of each FRET signal is dependent on relative labeling efficiencies for the two chaperone pools. (C) Glycerol gradient peak profiles are shown for histone complexes made with a double loop mutant of Np-A2 (AKDE to AGGG and K82S). (left) Smaller histone dimer complexes are formed with the interface mutant of Np-A2. (right) The Np-A2 interface mutant binds all four core histones to form large complexes. (D) A highly charged, double loop mutant of Np-A2 (AKDE to AGEE and K82E) binds histone dimers normally to form smaller complexes.

gradients. In this experiment, mutant Np-A2 chaperones formed large complexes with histone dimers and tetramers that were similar to wild-type complexes (Figure 4C, right). The double loop mutant of Np-A2 also formed normal complexes with H2A-H2B dimers by themselves (Figure 4C, left). We then monitored decamer formation with FRET using Np-A2 loop mutants labeled with donor or acceptor dyes. The addition of H2A-H2B dimers and H3-H4 tetramers to a mixture of the labeled Npm-A2 loop mutants gave a strong FRET signal, which suggests that chaperone decamers were formed in the complexes (Figure 4B, right). The addition of 1 M NaCl greatly reduced the FRET signal from the complexes, but was a bit less effective than expected, which may reflect some nonspecific aggregation of mutated chaperones in higher salt.

As a second test, we introduced a strong electrostatic repulsion into the interface between Np-A2 pentamers by re-engineering the AKDE loop to AGEE and replacing Lys82 with a glutamate residue (K82E). This Np-A2 double loop mutant was used to form complexes with histone dimers and tetramers. However, when the Np-A2 histone mixture in high salt (~1 M NaCl) was passed over a G25 desalting column to induce complex formation, the proteins aggregated and were bound to beads (not shown). In a parallel experiment, we found that this repulsive, double loop mutant of Np-A2 was able to bind H2A-H2B dimers normally (Figure 4D).

In summary, hydrogen bonds between residues in the AKDE and K-loops may not be strictly required for complex formation with all four core histones. Therefore, the critical step in assembling these larger complexes may be the ability of the H3-H4 tetramer to interact with H2A-H2B dimers on opposing chaperone pentamers and link them together. The AKDE to AGEE and K82E double loop mutant was designed to create a significant electrostatic repulsion in the interface between opposing pentamers. This prevented decamer formation by Np when binding the four core histones and led to aggregation, rather than a facile assembly of larger histone complexes. Finally, the observation that the repulsive double loop mutant of Np was able to form chaperone H2A-H2B complexes in a normal manner provides additional support for the idea that single pentamers form a central hub in these smaller histone complexes.[18]

Modeling an Npm2-Core Decamer. We next created a model of an Npm2-core decamer, since this species may represent an active form of the chaperone when it binds histone dimers and tetramers at the same time. It was hoped that the resulting model would show why critical loop residues in Npm2 have been changed relative to Np, with Asp58 going to Glu57 in the AKEE loop and Lys82 being replaced by Gln84 in the Q-loop. The Npm2-core decamer was modeled with a rigid body docking of two Npm2-core pentamers into the crystal structure of an Np-core decamer (pdb code: 1K5J). A side view of the modeled Npm2-core decamer is shown as a ribbon diagram (Figures 5A) and an electrostatic surface representation (Figure 5B). Note that A2- and A3-tracts in a full length Npm2 decamer would add 300 aspartate and glutamate residues in a charged cloud that envelops the chaperone. In addition, the 10 NLSs and KR regions would add about 190 lysine and arginine residues to partly neutralize this highly charged cloud.

Decamer formation by Np was shown previously to involve the formation of 5 pairs of water-mediated, hydrogen bonds involving Asp58 in the AKDE loop and Lys82 in the K-loop (Figure 5C).[9] In our model of the Npm2 decamer, the side chain of Glu57 was adjusted to an appropriate rotamer so that the distance between the carboxyl group and the side chain amino group of Gln84 in an opposing subunit is ~2.9 Å (Figure 5D). Thus, compensatory changes in these loop amino acids may allow a hydrogen bond to form directly between opposing Npm2 subunits, as occurs in human Npm1 decamers,[16] rather than relying on bridging water molecules, as seen in *Xenopus* Np and NO38 decamers.[9,11] Decamer formation may also be

dx.doi.org/10.1021/bi2006652 | *Biochemistry* 2011, 50, 8078–8089

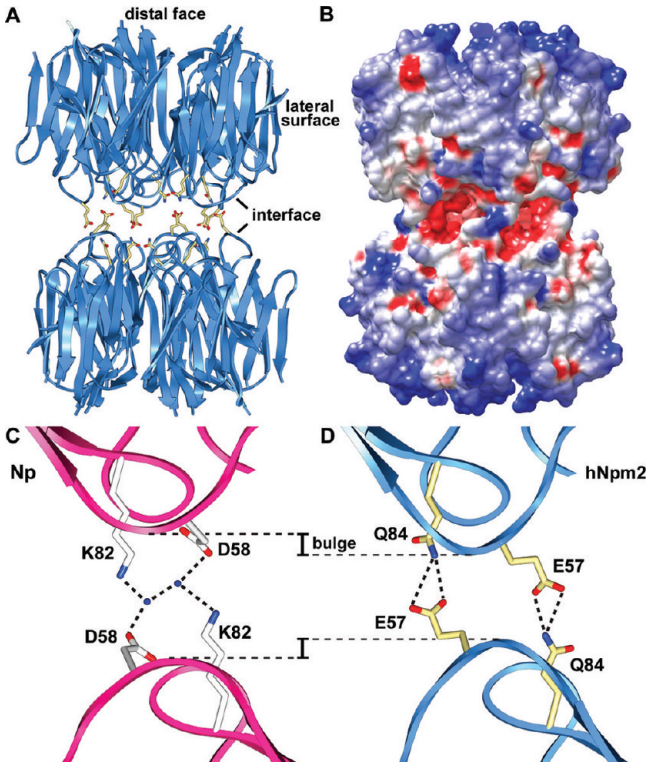

Figure 5. A decamer model for human Npm2-core. (A) A side view of a modeled Npm2-core decamer is shown as ribbons. Side chains of Glu57 and Gln84 within the interface are shown as sticks. (B) An electrostatic surface for the Npm2-core decamer is shown in a similar orientation as panel A. (C) A zoomed-in view is shown of two opposing Np subunits within the decamer interface. Residues in the AKDE (Asp58) and K-loops (Lys82) use water-mediated interactions to form a hydrogen-bonded network between opposing subunits.[9] (D) A simple rearrangement of the side chain of Glu57 in the AKEE-loop would allow the formation of hydrogen bonds between Glu57 and Gln84 in opposing subunits in the modeled Npm2 decamer. A bulge in the AKEE-loop moves the oppositely facing residues closer together (see dashed lines).

facilitated by a bulge that alters the path of the AKEE loop in Npm2 (Figure 1C), which places these loops ~2 Å closer together in the modeled decamer (see dashed lines in Figure 5C,D). This loop geometry may eliminate the necessity for bridging water molecules.

Finally, Lys56 of Npm2 is hydrogen bonded to Glu58 within the AKEE loop (Figure 1D). This interaction would position the Lys56 side chain to avoid electrostatic clashes within the interface between pentamers. A similar charge neutralization occurs between equivalent residues in AKDE loops (Lys57 and Glu59) of Np decamers.[9] In summary, the possible significance of an Npm2 decamer in binding core histones may be reflected by compensatory changes that have occurred in residues of the AKEE and Q-loops, along with overall changes in the geometry of AKEE loop.

Relative Histone Positions on Nucleoplasmin Decamers. Previously, we proposed that histone octamers may assemble on lateral surfaces of an Np decamer when core histones are bound.[9] Although Np is thought to be H2A-H2B specific,[5] the chaperone will bind H3-H4 tetramers to form large complexes.[11] To further our understanding of histone binding by nucleoplasmins, we evaluated the relative positions of H2A-H2B dimers and H3-H4 tetramers in the larger histone complexes. As a first step, we asked if Np-A2 forms decamers when the chaperone binds H3-H4 tetramers. In this experiment, separate pools of donor and acceptor labeled Np-A2 pentamers were mixed with histone tetramers. A strong FRET signal was observed when the ratio was optimized that is indicative of decamer formation (Figure 6A, left). This result is consistent with glycerol gradient analysis of the complexes.[11] We next asked whether the FRET signal between donor labeled Np-A2 and acceptor labeled histone tetramers would be maintained or reduced when of H2A-H2B dimers were also present. In this experiment, the measured FRET signal between H3-H4 tetramers and the chaperone was attenuated by ~40% when H2A-H2B dimers were present, after subtracting the background signal from Np-A2 (Figures 6A, middle, and 6B). This reduced FRET signal may be due to an additional spacing that has been introduced between donor dyes on the chaperone and acceptor dyes on H3-H4. This suggests that histone dimers are bound first to the chaperone followed by tetramers on the outside.

In a second experiment, we made complexes with donor labeled Np-A2 and acceptor labeled H2A-H2B dimers, in the absence or presence of H3-H4 tetramers. In this case, a strong FRET signal between Np and H2A-H2B dimers was significantly enhanced in the presence of H3-H4 (~1.6-fold; Figures 6A, right, and 6C). These data are consistent with the idea that histone dimers are bound directly to the chaperone and the increased FRET signal may arise from the effective dimerization of pentameric Np H2A-H2B complexes upon binding H3-H4 tetramers. In this scenario, DyLight 549 dye molecules on one Np pentamer may donate energy to DyLight 649 receptor dyes on H2A-H2B molecules bound to the adjacent pentamer, thereby enhancing the global FRET signal. When taken together, the FRET experiments and biochemical data are consistent with a sequential model of histone binding to nucleoplasmin. In this model, H2A-H2B dimers bind directly to Np pentamers. The addition of H3-H4 tetramers on the outside of these complexes then induces the formation of a chaperone decamer.[9]

DISCUSSION

Npm2: A Histone Chaperone. Three branches of the Np-family bind core histones, including the nucleoplasmins, dNLPs, and nucleophosmins.[9−11,28,29] Np assembles nucleosomes in an *in vitro* assay,[1,2,5,7,28] and Npm2 plays a significant role in maintaining heterochromatin architecture in oocytes and embryos.[3] In addition, Npm2 is required for the function of centromeric heterochromatin.[30] In this study, we show that human Npm2-A2 is able to bind core histones and form large complexes. Since Npm2 lacks the canonical A1-tract that is present in other Np-family members, the A2-tract is both necessary and sufficient for this chaperone to bind histones. In addition, the A3-tract in human and *Xenopus* nucleoplasmins is much smaller than the A2-tract and thus is likely to play an ancillary role in histone binding. On the basis of this data, we conclude that Npm2 may act as a histone chaperone in oocytes and early embryos. *Xenopus* Np is phosphorylated in oocytes on serine and threonine residues located within flexible N- and C-termini. The chaperone is then hyperphosphorylated in eggs prior to fertilization.[31−33] This markedly enhances the ability of Np to decondense sperm chromatin[32−36] and may allow the chaperone to remove linker histones from chromatin.[12] Since

dx.doi.org/10.1021/bi2006652 | *Biochemistry* 2011, 50, 8078−8089

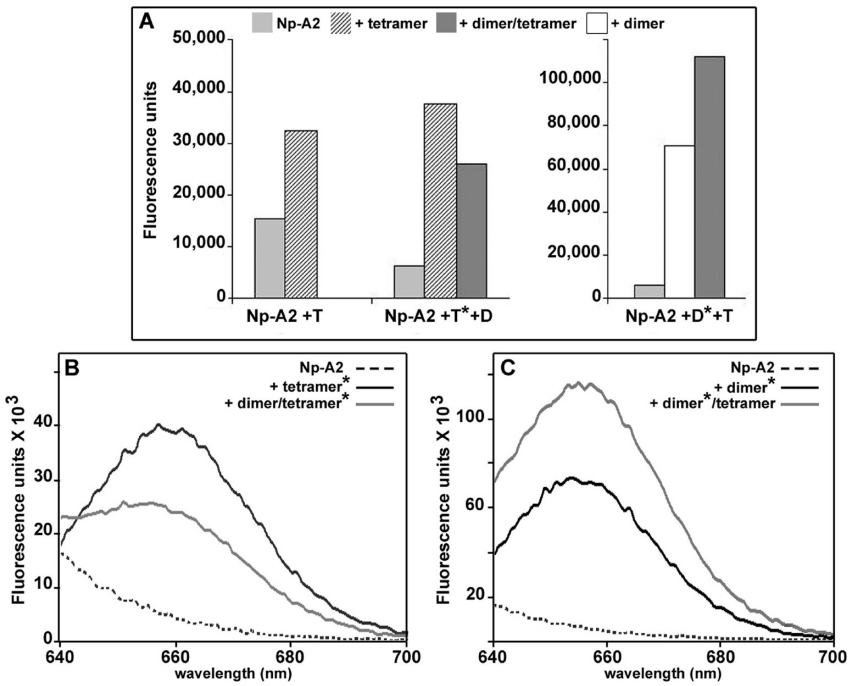

Figure 6. Sequential binding of histone dimers and tetramers to Np-A2 analyzed with FRET. (A) (left) Separately labeled Np-A2 pentamers containing donors or acceptors give a strong FRET peak when mixed with unlabeled histone tetramers, presumably due to decamer formation. (middle) Np-A2 pentamers labeled with donor molecules were mixed with acceptor labeled tetramers or a mixture of unlabeled dimers and labeled tetramers. The FRET signal from the Np-A2/tetramer coupling is diminished by ~40% when unlabeled histone dimers are present. (right) Acceptor labeled histone dimers were added to donor labeled Np-A2. A strong FRET signal occurred in the presence of added H2A-H2B dimers because they are bound directly to Np pentamers. The addition of unlabeled H3-H4 tetramers gave an enhanced FRET signal because twice as many labeled molecules are in close proximity within the decamer complex. (B) Fluorescence spectra are shown for the addition of histone dimers to a mixture of donor labeled Np-A2 and acceptor labeled H3-H4 tetramers, as summarized in panel A (middle). (C) Fluorescence spectra are shown for the experiment in panel A (right). Note the large increase in the FRET signal due to the addition of unlabeled histone tetramers to Np-A2/histone dimer complexes. An asterisk indicates the acceptor dye labeled ligand in each panel.

Npm2 is not required for sperm decondensation in knockout mice,[3] it is currently unclear whether Npm2 undergoes extensive phosphorylation.

Chaperone Pentamers and Decamers in Histone Binding. We have determined the structure of an Npm2 pentamer at 1.9 Å resolution to help define its role as a putative histone chaperone. Importantly, sequence conservation, structural data, and functional studies all suggest that Npm2 may bind core histones in a manner similar to Np. Thus, we propose that human and *Xenopus* nucleoplasmins bind H2A-H2B dimers on the lateral surfaces of their respective pentamers (Figure 7A, left and center panels). When H3-H4 tetramers are recruited, this results in a functional dimerization of the complex, such that chaperone decamers are formed with bound histone octamers (Figure 7A, right panel). In this model, nucleoplasmin pentamers and decamers may each form a central hub for bound histones depending upon their histone partners

In support of this model, we have shown that pentamers of Npm2 and Np each bind H2A-H2B dimers to form smaller complexes on glycerol gradients, when compared to chaperone complexes with the four core histones. Moreover, we did not observe a clear FRET signal between different pools of donor and acceptor labeled pentamers when H2A-H2B dimers were bound to human or *Xenopus* nucleoplasmins. We conclude that histone dimers bind to a chaperone pentamer (Figures 7B and 7C, left and middle panel), in agreement with low angle X-ray scattering experiments.[18] The five H2A-H2B dimers are probably bound to the lateral surface of an Np pentamer, with some contributions from A-1 tracts on the distal face.[18]

On the basis of previous data, we suggested that core histones may form octamers when they bind to Np decamers.[9] This idea is consistent with the apparent ratio of the core histones on Coomassie-stained SDS gels, coupled with molecular weight analysis of Np-complexes, which suggested that 5 histone octamers bind to an Np decamer (Figure 7C).[9] In this early work, we also suggested that histone dimers might bind to Np decamers, but solution X-ray scattering studies,[18] FRET data, and glycerol gradients now indicate that H2A-H2B dimers are bound to Np pentamers rather than to decamers. When H3-H4 tetramers are added to Np/H2A-H2B complexes, they do not displace histone dimers from the chaperone but instead are bound at a higher radius. This causes an effective dimerization of chaperone pentamers to form decamers. This process may reflect the ability of H3-H4 tetramers to interact with a pair of H2A-H2B dimers located on opposing chaperone pentamers in the decameric complex. This model is supported by FRET experiments that showed a significant increase in the signal between labeled Np-A2 and labeled H2A-H2B dimers when H3-H4 tetramers were added. This enhanced signal may be due to the close proximity of additional acceptor dyes to donor dyes in the larger complex. On the basis of our data, a similar assembly path may occur for Npm2 complexes with core histones (Figure 7B).

This data prompted us to model an Npm2-core decamer. Intriguingly, we found compensatory changes in residues of the

dx.doi.org/10.1021/bi2006652 | *Biochemistry* 2011, 50, 8078–8089

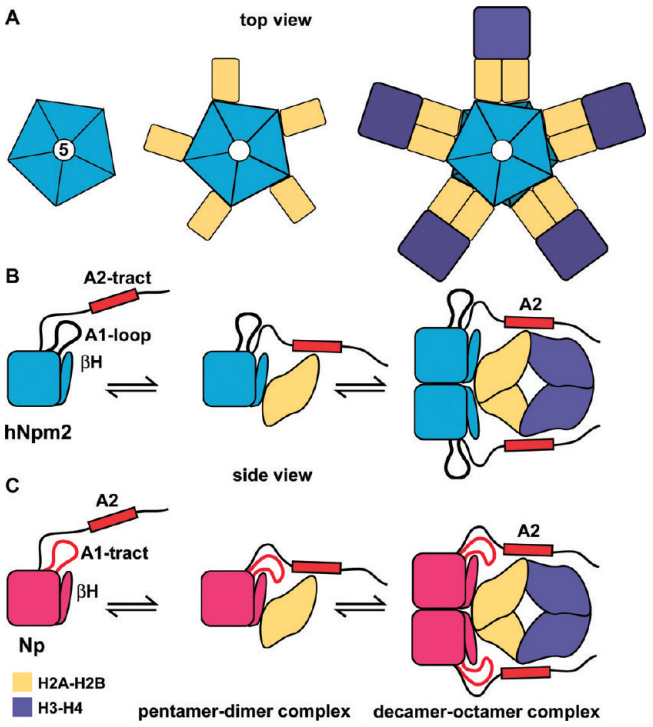

Figure 7. Models of histone binding by human and *Xenopus* nucleoplasmin. (A) Nucleoplasmin pentamers may bind histone dimers on their lateral surfaces. Subsequent binding of H3-H4 tetramers would form a bridge between two pentamer−histone dimer complexes. (B) A hypothetical, stepwise assembly of an Npm2 decamer/core histone complex is shown in a side view. This occurs when Npm2 pentamers bind a mixture of H2A-H2B dimers (gold) and H3-H4 tetramers (purple). The C-terminal A2-tract is required to form a stable histone complex and is shown schematically as a red rectangle, while the A1-loop (thick black line) is not required. For simplicity only 1 subunit in each Npm2 pentamer is shown and additional domains in the C-terminal tail are not shown in this figure. (C) Np decamers create a central hub when they bind a mixture of H2A-H2B dimers (gold) and H3-H4 tetramers to form histone octamers on the chaperone. Both the A1-tract (in red) and A2-tracts (red rectangle) help stabilize the complex.

AKEE and Q-loops. Thus, Lys82 in the K-loop of Np has been replaced by Gln84 with its shorter side chain in Npm2, while Asp58 in the AKDE loop of Np has been replaced by Glu57 with a longer side chain. The reciprocal nature of this dual substitution would allow 10 hydrogen bonds to form in the interface between pentamers. While the precise interface geometry in these large histone complexes is not known, it could be altered by histone binding. This may squeeze waters out of the relatively open interface,[9,17] as observed in the human Npm1 decamer.[16] To test the role of the AKDE and K-loops, salt bridge forming residues were mutated to residues with smaller, uncharged side chains. Remarkably, this double loop mutant of Np-A2 did not lose its ability to bind core histones. Hence, cooperative binding of core histones on the lateral surface of the decamer may drive formation of the larger complexes in the absence of these salt bridges (Figure 7A−C, right panel). However, a highly repulsive, double loop mutant (AKDE to AGEE and K82E) disrupted the formation of Np complexes with the four core histones, while complexes with histone dimers formed normally. This lends further support to the idea that the chaperone decamer plays an important role in binding the four core histones and is consistent with a model in which H2A-H2B dimers bind to single pentamers.

The ability of chaperone pentamers and decamers to each form central hubs for histone binding can be reconciled if H2A-H2B dimers bind in a similar way in both complexes (Figure 7A−C, middle and right panels). Thus, depending upon local protein concentration and binding partners, nucleoplasmins may bind histones as a pentamer (Figure 7A, middle panel) or a decamer (Figure 7A, right panel). In fact, Np is one of the most abundant proteins in oocyte nuclei where it is present at ∼5 mg/mL.[5,6,38] Hence, the high local nuclear concentration of the chaperone might favor decamer formation *in vivo* when H2A-H2B dimers are bound, especially if the effects of molecular crowding are factored in. At this point it is not clear whether Np may bind histone dimers and tetramers simultaneously *in vivo*. Given the high concentration of histones and chaperones in *Xenopus* oocytes,[38,39] it is possible that larger histone complexes may be formed, which subsequently disassociate upon purification due to dilution. Further studies are now needed on this point.

An alternative model of H2A-H2B binding has recently been proposed that was based on a low-resolution EM map of egg Np with bound dimers. This study showed additional density for histone dimers on the distal surface of hyper-phosphorylated Np pentamers.[19] However, histone−chaperone complexes may not be particularly stable under the harsh conditions of negative staining with uranyl acetate (high salt and low pH). We suggest that sample preparation may have caused a local rearrangement of basic H2A-H2B dimers onto the acidic crown, located on the distal surface of hyperphosphorylated Np pentamers. Moreover, data on negatively stained complexes disagree with solution X-ray scattering[18] and contradict a large body of biochemical and FRET data (this work).[9,11] Further studies are now needed to clarify this issue.

Acidic Tracts in Histone Binding. Npm2 and Np use tracts of acidic residues in histone binding. For Npm2, the A2-tract is sufficient to bind core histones because the A1-loop contains only a single acidic residue (Figure 7B). Intriguingly, Npm2 is the only family member that does not have a canonical A1-tract of 3−12 acidic residues.[9] The lack of this acidic loop correlates with the inability of Npm2-core pentamers to bind histones. Loop exchange experiments showed that histone binding by Npm2-core was not rescued by replacing its A1-loop with the much more acidic loop from Np. Hence, reverse engineering the Npm2-core to bind histones efficiently was not a simple task, presumably due to other changes in surface residues of Npm2. In particular, the surface of the Npm2-core pentamer is much more basic than its Np counterpart.

When the A1-tract of Np was replaced with the A1-loop from human Npm2, the Np-core pentamer lost its ability to form normal histone complexes. This observation supports the idea that the A1-tract in Np must play an important role in binding core histones.[14] Indeed, Np uses both A1- and A2-tracts for histone binding (Figure 7C).[9] In general, the A1-tract is quite flexible in Np-family members (this work).[9−11,16] Thus, each pentamer in the Np-family (except Npm2) contains a flexible, acidic crown on its distal surface composed of five A1-tracts that can participate in histone binding. Our data further suggest that the A2-tract of Npm2 is sufficient to direct histone binding, whereas the A2-tract of Np may act synergistically with the A1-tract to form histone complexes. Mechanistically, the lack of a functional A1-tract in Npm2 argues against the idea that core histones bind exclusively to the distal or (top) surfaces of the

dx.doi.org/10.1021/bi2006652 | *Biochemistry* 2011, 50, 8078−8089

pentamer under physiological conditions[19] because there is no acidic crown in this chaperone. A more parsimonious model is possible for histone binding to nucleoplasmins. In this case, histones interact mostly with the lateral surface of a pentamer or decamer, with flexible A1-tracts in Np playing an important role in histone binding. At the same time, additional interactions between flexible A2-tracts and basic histones would stabilize the complexes (Figure 7B,C).

Finally, Npm2 and Np chaperones are direct orthologs yet they differ in one important respect. Sperm decondensation proceeds normally in Npm2 knockout mice,[3] while Np is required to remodel sperm chromatin in *Xenopus* eggs.[13−15,32−36,40] This chromatin remodeling process depends upon the A1 and A2 tracts of Np, which may remove sperm basic proteins from highly condensed chromatin. This is followed by a second step in which core histones are delivered to DNA.[14,40] Npm2 does not have a functional A1-tract which may impede its ability to function in the first step of sperm chromatin decondensation. This suggests that another chaperone may assume this role in mammalian eggs. Even so, it is possible that Npm2 may deliver histones to DNA during sperm chromatin remodeling.

■ ASSOCIATED CONTENT

Ⓢ Supporting Information

Figure 1. This material is available free of charge via the Internet at http://pubs.acs.org.

Accession Codes

Coordinates for two hNpm2-core pentamers (3T30) have been deposited in the PDB.

■ AUTHOR INFORMATION

Corresponding Author

*E-mail: cakey@bu.edu. Phone: 617 638 4051. Fax: 617 638 4041.

Author Contributions

†These authors contributed equally to the work.

Funding

This work was carried out with grant support from the NIH to C.W.A. (R01-GM060537).

■ ACKNOWLEDGMENTS

We thank Martin Matzuk for the original hNpm2 expression vector and personnel at beamline X8C at the NSLS for help with data collection.

■ ABBREVIATIONS

Npm2, human nucleoplasmin; Np, *Xenopus* nucleoplasmin; Npm2- and Np-core, N-terminal domains of Npm2 and Np; Npm2-A2 and Np-A2, chaperones with a second large acidic tract (A2) in the C-terminal tail; core histones, equimolar mixture of H2A-H2B and H3-H4; AMS, ammonium sulfate.

■ REFERENCES

(1) Laskey, R. A., Honda, B. M., Mills, A. D., and Finch, J. T. (1978) Nucleosomes are assembled by an acidic protein which binds histones and transfers them to DNA. *Nature 275*, 416−420.

(2) Philpott, A., and Laskey, R. A. (2000) Nuclear chaperones. *Semin Cell Dev. Biol. 11*, 7−14.

(3) Burns, K. H., Viveiros, M. M., Ren, Y., Wang, P., DeMayo, F. J., Frail, D. E., Eppig, J. J., and Matzuk, M. M. (2003) Roles of NPM2 in chromatin and nucleolar organization in oocytes and embryos. *Science 300*, 633−636.

(4) Ye, X., Franco, A. A., Santos, H., Nelson, D. M., Kaufman, P. D., and Adams, P. D. (2003) Defective s-phase chromatin assembly causes DNA damage, activation of the s-phase checkpoint, and s-phase arrest. *Mol. Cell 11*, 341−351.

(5) Kleinschmidt, J. A., Fortkamp, E., Krohne, G., Zentgraf, H., and Franke, W. W. (1985) Co-existence of two different types of soluble histone complexes in nuclei of Xenopus laevis oocytes. *J. Biol. Chem. 260*, 1166−176.

(6) Kleinschmidt, J. A., Dingwall, C., Maier, G., and Franke, W. W. (1986) Molecular characterization of a karyophilic, histone-binding protein: cDNA cloning, amino acid sequence and expression of nuclear protein N1/N2 of Xenopus laevis. *EMBO J. 5*, 3547−3552.

(7) Zucker, K., and Worcel, A. (1990) The histone H3/H4.N1 complex supplemented with histone H2A-H2B dimers and DNA topoisomerase I forms nucleosomes on circular DNA under physiological conditions. *J. Biol. Chem. 265*, 14487−14496.

(8) Robbins, J., Dilworth, S. M., Laskey, R. A., and Dingwall, C. (1991) Two interdependent basic domains in nucleoplasmin nuclear targeting sequence: identification of a class of bipartite nuclear targeting sequence. *Cell 64*, 615−623.

(9) Dutta, S., Akey, I. V., Dingwall, C., Hartman, K. L., Laue, T., Nolte, R. T., Head, J. F., and Akey, C. W. (2001) The crystal structure of nucleoplasmin-core: implications for histone binding and nucleosome assembly. *Mol. Cell 8*, 841−853.

(10) Namboodiri, H. V. M., Dutta, S., Akey, I. V., Head, J. F., and Akey, C. W. (2003) The crystal structure of Drosophila NLP-core provides insight into pentamer formation and histone binding. *Structure 11*, 175−86.

(11) Namboodiri, H. V. M., Akey, I. V., Schmidt-Zachmann, M. S., Head, J. F., and Akey, C. W. (2004) Structure and function of Xenopus NO38-core, a histone chaperone in the nucleolus. *Structure 12*, 2149−2160.

(12) Ramos, I., Prado, A., Finn, R. M., Muga, A., and Ausió, J. (2005) Nucleoplasmin-mediated unfolding of chromatin involves the displacement of linker-associated chromatin proteins. *Biochemistry 44*, 8274−8281.

(13) Hierro, A., Arizmendi, J. M., De Las Rivas, J., Urbaneja, M. A., Prado, A., and Muga, A. (2001) Structural and functional properties of Escherichia coli-derived nucleoplasmin. A comparative study of recombinant and natural proteins. *Eur. J. Biochem. 268*, 1739−1748.

(14) Salvany, L., Chiva, M., Arnan, C., Ausió, J., Subirana, J. A., and Saperas, N. (2004) Mutation of the small acidic tract A1 drastically reduces nucleoplasmin activity. *FEBS Lett. 576*, 353−357.

(15) Taneva, S.G., Muñoz, I. G., Franco, G., Falces, J., Arregi, I., Muga, A., Montoya, G., Urbaneja, M. A., and Bañuelos, S. (2008) Activation of nucleoplasmin, an oligomeric histone chaperone, challenges its stability. *Biochemistry 47*, 13897−13906.

(16) Lee, H. H., Kim, H. S., Kang, J. Y., Lee, B. I., Ha, J. Y., Yoon, H. J., Lim, S. O., Jung, G., and Suh, S. W. (2007) Crystal structure of human nucleophosmin-core reveals plasticity of the pentamer-pentamer interface. *Proteins 69*, 672−678.

(17) Akey, C. W., and Luger, K. (2003) Histone chaperones and nucleosome assembly. *Curr. Opin. Struct. Biol. 13*, 6−14.

(18) Taneva, S.G., Bañuelos, S., Falces, J., Arregi, I., Muga, A., Konarev, P. V., Svergun, D. I., Velázquez-Campoy, A., and Urbaneja, M. A. (2009) A mechanism for histone chaperoning activity of nucleoplasmin: thermodynamic and structural models. *J. Mol. Biol. 393*, 448−463.

(19) Ramos, I., Martín-Benito, J., Finn, R., Bretaña, L., Aloria, K., Arizmendi, J. M., Ausió, J., Muga, A., Valpuesta, J. M., and Prado, A. (2010) Nucleoplasmin binds histone H2A-H2B dimers through its distal face. *J. Biol. Chem. 285*, 33771−33778.

(20) Studier, F. W. (2005) Protein production by auto-induction in high density shaking cultures. *Protein Expr. Purif. 41*, 207−234.

(21) Luger, K., Rechsteiner, T. J., Flaus, A. J., Waye, M. M., and Richmond, T. J. (1997) Characterization of nucleosome core particles containing histone proteins made in bacteria. *J. Mol. Biol. 272* (3), 301−11.

(22) Otwinowski, Z., and Minor, W. (1997) Processing of X-ray diffraction data collected in oscillation mode. *Methods Enzymol. 276*, 307−326.

(23) Kissinger, C. R., Gehlhaar, D. K., and Fogel, D. B. (1999) Rapid automated molecular replacement by evolutionary search. *Acta Crystallogr., Sect. D: Biol. Crystallogr. 55*, 484−491.

(24) Brunger, A. T., Adams, P. D., Clore, G. M., DeLano, W. L., Gros, P., Grosse-Kunstieve, R. W., Jiang, J. S., Kuszewski, J., Nilges, M., Pannu, N. S., Read, R. J., Rice, L. M., Simonson, T., and Warren, G. L. (1998) Crystallography and NMR system (CNS): a new software suite for macromolecular structure determination. *Acta Crystallogr., Sect. D: Biol. Crystallogr. 54*, 905−921.

(25) Emsley, P., and Cowtan, K. (2004) Coot: Model-building tools for molecular graphics. *Acta Crystallogr., Sect. D: Biol. Crystallogr. 60*, 2126−2132.

(26) Adams, P. D., Grosse-Kunstleve, R. W., Hung, L. W., Ioerger, T. R., McCoy, A.J., Moriarty, N. W., Read, R. J., Sacchettini, J. C., Sauter, N. K., and Terwilliger, T. C. (2002) PHENIX: building new software for automated crystallographic structure determination. *Acta Crystallogr., Sect. D: Biol. Crystallogr. 58*, 1948−1954.

(27) Laskowski, R. A., MacArthur, M. W., Moss, D. S., and Thornton, U. M. (1993) PROCHECK: a program to check the stereochemical quality of protein structures. *J. Appl. Crystallogr. 26*, 283−291.

(28) Ito, T., Tyler, J. K., Bulger, M., Kobayashi, R., and Kadonaga, J. T. (1996) ATP-facilitated chromatin assembly with a nucleoplasmin-like protein from Drosophila melanogaster. *J. Biol. Chem. 271*, 25041−25048.

(29) Okuwaki, M., Iwamatsu, A., Tsujimoto, M., and Nagata, K. (2001) Function of nucleophosmin/B23, a nucleolar acidic protein, as a histone chaperone. *FEBS Lett. 506*, 272−276.

(30) De La Fuente, R., Viveiros, M. M., Burns, K. H., Adashi, E. Y., Matzuk, M. M., and Eppig, J. J. (2004) Major chromatin remodeling in the germinal vesicle (GV) of mammalian oocytes is dispensable for global transcriptional silencing but required for centromeric heterochromatin function. *Dev. Biol. 275*, 447−458.

(31) Cotten, M., Sealy, L., and Chalkley, R. (1986) Massive phosphorylation distinguishes Xenopus laevis nucleoplasmin isolated from oocytes or unfertilized eggs. *Biochemistry 25*, 5063−5069.

(32) Bañuelos, S., Hierro, A., Arizmendi, J. M., Montoya, G., Prado, A., and Muga, A. (2003) Activation mechanism of the nuclear chaperone nucleoplasmin: role of the core domain. *J. Mol. Biol. 334*, 585−593.

(33) Bañuelos, S., Omaetxebarria, M. J., Ramos, I., Larsen, M. R., Arregi, I., Jensen, O. N., Arizmendi, J. M., Prado, A., and Muga, A. (2007) Phosphorylation of both nucleoplasmin domains is required for activation of its chromatin decondensation activity. *J. Biol. Chem. 282*, 21213−21221.

(34) Leno, G. H., Mills, A. D., Philpott, A., and Laskey, R. A. (1996) Hyperphosphorylation of nucleoplasmin facilitates Xenopus sperm decondensation at fertilization. *J. Biol. Chem. 271*, 7253−7256.

(35) Philpott, A., Leno, G. H., and Laskey, R. A. (1991) Sperm decondensation in Xenopus egg cytoplasm is mediated by nucleoplasmin. *Cell 65*, 569−578.

(36) Philpott, A., and Leno, G. H. (1992) Nucleoplasmin remodels sperm chromatin in Xenopus egg extracts. *Cell 69*, 759−767.

(37) Goddard, T. D., Huang, C. C., and Ferrin, T. E. (2005) Software extensions to UCSF chimera for interactive visualization of large molecular assemblies. *Structure 13*, 473−482.

(38) Kleinschmidt, J. A., Seiter, A., and Zentgraf, H. (1990) Nucleosome assembly in vitro: separate histone transfer and synergistic interaction of native histone complexes purified from nuclei of *Xenopus laevis* oocytes. *EMBO J. 9*, 1309−1318.

(39) Woodland, H. R., and Adamson, E. D. (1977) The synthesis and storage of histones during the oogenesis of *Xenopus laevis*. *Dev. Biol. 57*, 118−135.

(40) Hierro, A., Arizmendi, J. M., Bañuelos, S., Prado, A., and Muga, A. (2002) Electrostatic interactions at the C-terminal domain of nucleoplasmin modulate its chromatin decondensation activity. *Biochemistry 41*, 6408−6413.